

Study on Gas Adsorption–Desorption and Diffusion Behaviour in Coal Pores Modified by Nano Fracturing Fluid

Wei qin Zuo, Mingrui Qi, Yanwei Liu, Huaizhen Li,* Hongkai Han, Yang Wang, Liquan Long, and Shengjie Wu



Cite This: *ACS Omega* 2023, 8, 29213–29224



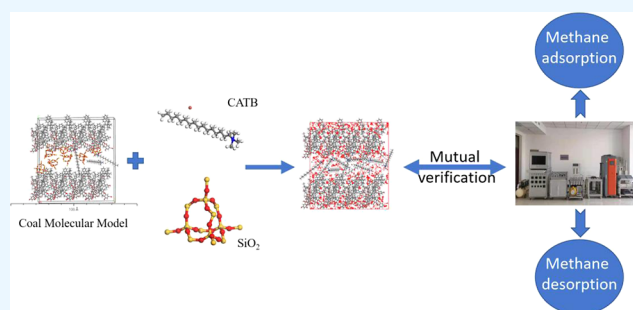
Read Online

ACCESS |

Metrics & More

Article Recommendations

ABSTRACT: Nanoparticles are added to clean fracturing fluids to formulate nanoparticle-modified clean fracturing fluids, compared with ordinary clean fracturing fluid, it has the advantages of good temperature resistance, low loss of filtration, and so forth, and has good application prospects in coal-bed methane. However, the current research on nanoparticle-modified clean fracturing fluids is mostly focused on the study of their rheological properties. The mechanism of nano-fracturing fluid influence on methane adsorption–desorption characteristics is not clear. Therefore, this study chooses Jiulishan anthracite coal (high-rank coal), Pingdingshan coal (medium-rank coal), and Geng village mine long bituminous coal (low-rank coal) of the three rank coal samples. Using indoor experiments and molecular simulation methods, a study on the influence of methane adsorption and desorption capacity and diffusion ability of coal samples provides a modified fracturing fluid formulation of 0.8% CATB + 0.2% NaSal + 1% KCl + SiO₂. The experimental results show that nanofracturing fluid-treated coal samples compared to clean fracturing fluid treated coal samples, both methane adsorption and desorption capacities, were increased to some extent. Construction of methane adsorption systems with different apertures and calculation of isosteric heat of adsorption, indicating that the interaction force between methane and coal molecules is smaller after nanofracturing fluid treatment, which facilitated methane desorption. A simulation study of methane diffusion in coal samples treated with two systems of fracturing fluids at different aperture was carried out using molecular dynamics methods, indicating that nanoparticle-modified clean fracturing fluids can reduce the damage of clean fracturing fluids to the desorption–diffusion ability of coal reservoirs. Comparison of 6 MPa as the most suitable pressure for nanofracturing fluids to function provides a basis for the future development of nanofracturing fluids and their popularization.



1. INTRODUCTION

Coalbed methane is a self-generated, self-storage unconventional natural gas stored in coal seams and is a high-quality clean energy source and fossil fuel. China's coal-bed methane resources are abundant and have a broad space for development, with coalbed methane reserves below 2000 m burial depth of about 36.81 trillion m³.¹ Vigorously promoting coalbed methane mining not only can solve the problem of China's energy shortage but also can protect China's energy security, ensure the safe production of coal mining, and curb coal mine gas disaster. Coalbed methane is stored in coal seams and most of it exists in the form of adsorbed state, which accounts for about 80% of coalbed methane content. China's coalbed methane mining industry is developing rapidly, but most of the coal reservoirs have the characteristics of “three lows” and also have strong heterogeneity, which brings a lot of difficulties to coalbed methane mining.^{2,3} Fracturing technology has been proven to be the most effective method for extracting coalbed methane.^{4,5} Fracturing uses high pressure to open a fracture in

the coal seam, and then the fracturing fluid carries the proppant into the coal seam to achieve the effect of extracting CBM. As an important medium for fracturing and carrying proppant, scholars have not stopped studying the performance of fracturing fluid since its introduction.^{6,7} Clean fracturing fluid were prepared with gemini antistatic agent SN as surfactant, sodium salicylate and potassium chloride as salts, modification of clean fracturing fluids with nanoscale barium titanate, silicon dioxide, graphite, and carbon nanotubes, respectively, and testing the change of rheological properties of modified clean fracturing fluids. The results showed that the addition of appropriate volume fractions of barium titanate,

Received: April 13, 2023

Accepted: July 26, 2023

Published: August 3, 2023



silica, and graphite at 30 °C could enhance the shear viscosity of clean fracturing fluid, and it was also found that the shear viscosity was affected by the material, particle size, and addition percentage of nanoparticles.⁸ Three surfactants were used to modify coal samples of different coal grades and then tested the contact angle of the modified coal samples. It was found that the contact angle of the modified coal changed significantly with increasing coal grades; the adsorption density of the three surfactants decreased and thus a surfactant adsorption model was proposed.⁹ Addition of silicon dioxide with a diameter of 30 nm to an aqueous solution of hexadecyl trimethyl ammonium bromide and sodium nitrate and used rheology and low-temperature transmission electron microscopy to test the effect of nanoparticles added at 1% volume fraction on the shear rate and relaxation time of the solutions, the test results show that the nanoparticles can enhance the shear rate of the mixed solution, increase the relaxation time and interact with the mixed solution to form micelles.¹⁰ In the simulation study of CO₂ sequestration in coal seams by building a molecular model of bituminous coal, it was found that CO₂ is more easily adsorbed by coal and CO₂ can obtain more pore space than CH₄, and the adsorption of CO₂ can cause the expansion of coal structure at a certain amount.¹¹ The molecular structure of coal obtained by ¹³C NMR was continuously adjusted, corrected using molecular simulation software, and carried out binary isothermal adsorption simulations on the final model, showing that CO₂ is more competitive than CH₄ for adsorption.¹² The effects of nanofluids on the microporous structure of CBM reservoirs were studied in several aspects by nuclear magnetic resonance (NMR) experiments, low-temperature liquid nitrogen adsorption experiments, and contact angle experiments. The effects of different adsorption mechanisms of TiO₂ nanoparticles on the surface wettability of rock samples were analyzed, and it was found that the adsorption of particles was beneficial to enhance the water wettability of the pore throat surface and to reduce the damage to water lock.¹³

Most studies on nanoparticle-modified clean fracturing fluids have been conducted on fracturing fluid testing the physical properties of nanoparticle addition on clean fracturing fluid rheological properties, zero-shear viscosity, sand-carrying properties, and control of particle transport in sandstone reservoirs, with a lack of nanoparticle-modified clean fracturing fluid effects on coal adsorption and desorption of methane. To address this issue, this paper uses nanoparticle-modified clean fracturing fluid to treat low-, medium- and high-rank coal samples to investigate the effect of nanoparticle-modified clean fracturing fluid on coal adsorption and desorption methane ability, to verify the regular from the experiments with molecular simulation software, and to provide guidance for the development of nanoparticle-modified clean fracturing fluid.

2. EXPERIMENTS AND METHODS

2.1. Experiment Preparation. When the size of small particles is reduced to the nanometer scale (1~100 nm), these particles demonstrate their own small size effect, surface effect, quantum size effect, and macroscopic quantum and tunneling effects; thus, this change can exhibit many unique properties, which have promising applications as catalysis and new materials and in light filtering, light absorption, medicine.¹⁴ To investigate the effect of addition of Cu²⁺ nanoparticles with different volume fractions on the thermal conductivity and

viscosity of viscoelastic surfactant solutions (hexadecyl trimethyl ammonium chloride and sodium salicylate). The results showed that the larger the volume fraction of Cu²⁺, the higher the thermal conductivity of the nano-viscoelastic solution. The temperature had a large effect on the viscosity of the nano-viscoelastic solution when the volume fraction of Cu²⁺ added was larger, and the viscosity decreased when the temperature was higher. Conversely, temperature had little effect on the viscosity when the volume fraction of Cu²⁺ was smaller.¹⁵ Nanofluids were prepared from multiwalled carbon nanotubes with hexadecyl trimethyl ammonium bromide and sodium salicylate to investigate the effect of the volume fraction of carbon nanotubes added on the shear viscosity of nanofluids, and the results showed that shear viscosity was positively correlated with the volume fraction of nanoparticles and negatively correlated with temperature.¹⁶

The nanofracturing fluid required for this experiment is formulated on top of the clean fracturing fluid, and the formula of this clean fracturing fluid is 0.8% hexadecyl trimethyl ammonium bromide (CATB) + 0.2% NaSal + 1% KCl. It has been shown that the shear viscosity, sand-carrying properties, and gel-breaking properties of nanofracturing fluids prepared by adding nano-silica to clean fracturing fluids are enhanced. Therefore, in this paper, nano-silica was selected to modify the clean fracturing fluid for preparation, nanoparticle-modified fracturing fluid was made, and the mass fraction of nano-silica addition was added at 0.5, 1, and 1.5%.

The coal samples with three degrees of metamorphism were taken from the fresh coal walls of three mines, namely, anthracite (high-rank), coking coal (middle-rank), and long bituminous coal (low-rank), at Jiaozuo Jiulishan coal mine, Pingdingshan eighth mine, and Sanmenxia Geng Village coal mine in Henan Province.

A portion of each of the three coal samples was collected from the newly collected coal samples, crushed through a grinder, and sieved into coal samples with a particle size of 1–3 mm for the experiment. Each coal sample was sieved by approximately 2 kg, and after sieving, it was put into a sealed bag with a label to be prepared.

Preparation of coal samples for experiments on the effect of nanofracturing fluid on methane adsorption and desorption capacity was completed as follows. (1) Formulation of modified fracturing fluids containing 0.5, 1, and 1.5% nanoparticles and fracturing fluids without nanoparticles were used as controls. (2) Three beakers were used to place the prepared coal samples, with 800 g of sample placed into each beaker. (3) Pour 200 mL of prepared modified fracturing fluid into each beaker, stir with a glass rod, fully contact the coal with the fracturing fluid, and let it rest for 48 h. (4) Remove the supernatant, pour the coal sample with the lower layer of modified fracturing fluid into the tray, and put it into the vacuum drying oven set to 100 °C for drying; then, allow the samples to dry for 24 h. (5) Remove the tray after drying is completed, then put the coal samples into sealed bags with labels after they have cooled to room temperature.

2.2. Experimental Protocol and Instrumentation. To study the effect of nano clean fracturing fluid on the methane adsorption and desorption capacity of different coal rank coals, the prepared coal samples of different coal ranks need to be loaded into a closed coal sample tank, filled with a certain amount of methane, and adsorbed over a period of time to reach adsorption equilibrium; then, the pressure values of the buffer tank before and after adsorption equilibrium are

recorded for each group of experimental coal samples in turn. After equilibrium is achieved, the pressure is quickly relieved such that the pressure gauge of the coal sample tank drops to 0. Immediately, the valve of the desorber is opened, and the measured gas desorption volume at different time points is measured using the drainage collection method. The experiment used to study the effect of clean fracturing fluid action on coal methane adsorption–desorption capacity using a gas adsorption–desorption experimental apparatus was developed by the Safety College of Henan Polytechnic University. The experimental apparatus is mainly composed of four parts: an inflation unit, a constant temperature water bath unit, a vacuum degassing unit, and an automatic gas diffusion measurement device. The experimental apparatus is shown in Figure 1.



Figure 1. Physical diagram of the gas adsorption–desorption experimental instrument (Photograph courtesy of Yang Wang, Copyright 2022).

The molecular simulation study of coal rock pore methane adsorption diffusion was completed using Materials Studio simulation software to construct the minimum energy and optimal density raw coal molecular model; the different pore sizes were established with a coal slit pore model, using coal adsorption fracturing fluid as the entry point to solve the problem; the clean fracturing fluid and manufacturing fluid treated were constructed using a coal molecular structure model; then, methane adsorption and diffusion simulations were carried out, and the adsorption and diffusion coefficients of methane after treatment with clean fracturing fluid and nanofracturing fluid were calculated, and the change patterns of methane adsorption and diffusion coefficients before and after nanofracturing fluid treatment were derived.

3. RESULTS AND DISCUSSION

3.1. Effect of Nano Fracturing Fluids on the Adsorption–Desorption Capacity of Coal for Gas. Coal is a porous medium with a large specific surface area and a high adsorption capacity for coalbed methane. There are two forms of coalbed methane in coal reservoirs: the free and the adsorbed state. The adsorbed CBM accounts for more than 80% of the CBM content in coal reservoirs and most of the CBM in coal reservoirs exists mainly in the form of physical adsorption in coal pores. The extraction of coalbed methane in coal reservoirs is a dynamic process that includes desorption, diffusion, and gas percolation of the coalbed methane.¹⁷ Therefore, suppressing coalbed methane adsorption and promoting coalbed methane desorption are important measures that improve the coalbed methane extraction effect.

In the following paper, isothermal adsorption–desorption experiments of coal under the action of nanofracturing fluid are conducted using a gas adsorption–desorption experimental apparatus to investigate the effect of nanofracturing fluid on the ability of coal to adsorb–desorb gas.

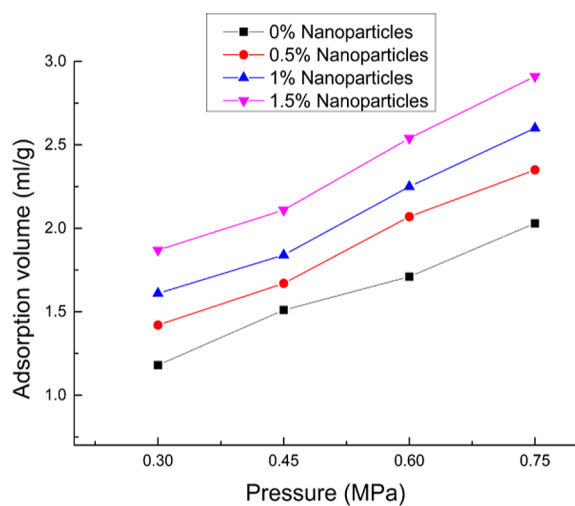
3.1.1. Isothermal Adsorption Experiments and Data Analysis. From the three different coal samples prepared, 800 g of each coal sample was used to conduct isothermal adsorption experiments as follows:

- ① The airtightness of the device was checked, and the remaining space volume of the coal sample tank was measured. The constant temperature water bath and vacuum pump were turned on, and the temperature of the constant temperature water bath was set to 60 °C.
- ② The valve of the coal sample tank and the valve of the vacuum pump was opened, the switch of the vacuum pump was turned on, the coal sample was degassed, and the degas time reached 12 h or more.
- ③ The temperature of the constant temperature water was adjusted to the 30 °C; then, the valve of the high-pressure gas cylinder and the valve of the buffer tank were unscrewed; then, the high-pressure gas cylinder and the buffer tank were connected and allowed to slowly fill with methane gas waiting until the gas pressure of the buffer tank is approximately three times the target adsorption equilibrium pressure of the coal sample tank; finally, the valve of the high-pressure gas cylinder was closed, and the pressure value of the buffer tank after the pressure stabilizes was recorded.
- ④ The valve of the coal sample tank was slowly opened to allow the methane in the buffer tank to enter the coal sample tank, and the starting filling time and the change value of the pressure gauge of the buffer tank were recorded for each filling. The set adsorption equilibrium pressure was reached after more than 12 h of repeated filling. Generally, the gas pressure in the coal sample tank did not drop more than 0.01 MPa per hour, which indicates that the coal sample has reached the adsorption equilibrium state, and finally, the adsorption amount is calculated.

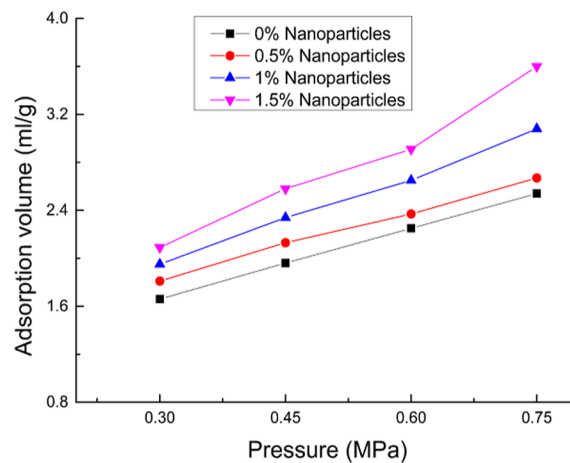
Figure 2 shows the adsorption amounts measured at 0.3, 0.45, 0.6, and 0.75 MPa for three coal rank coal samples at 30 °C.

From Figure 2 and Table 1, the methane adsorption amount of the three different coal rank coal samples treated with normal clean fracturing fluid and nanofracturing fluid showed an increasing trend with increasing pressure. The results of methane isothermal adsorption experiments showed that the methane adsorption amounts of coal samples treated with different mass fraction nanofracturing fluids were higher than those treated with normal clean fracturing fluids. At an adsorption equilibrium pressure of 0.75 MPa, the nanoparticle mass fractions were 0.5, 1.0, and 1.5% compared to the methane adsorption of coal samples after treatment with normal clean fracturing fluid, the increase of gas adsorption for low-rank coal was 15.76, 10.63, and 11.92%, and the increase of gas adsorption for middle-rank coal was 5.12, 11.36, and 18.50%, respectively; the increase of gas adsorption for high-rank coal was 23.55, 5.45, and 3.87%, respectively.

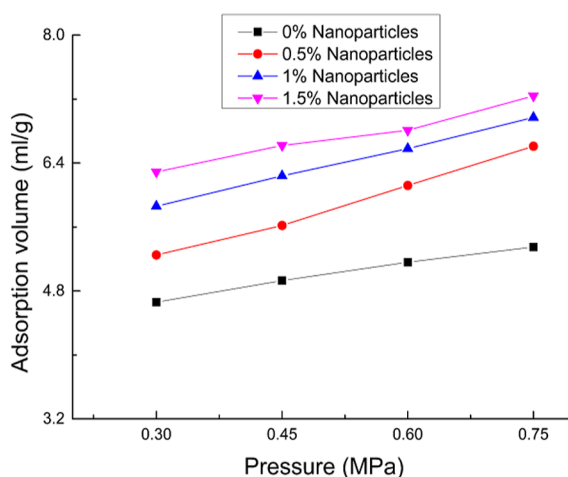
3.1.2. Isothermal Desorption Experiments and Data Analysis. When the coal sample adsorption reached equilibrium, the water temperature and atmospheric pressure in the



a. Adsorption capacity of low-rank coal



b. Adsorption capacity of medium-rank coal



c. Adsorption capacity of high-rank coal

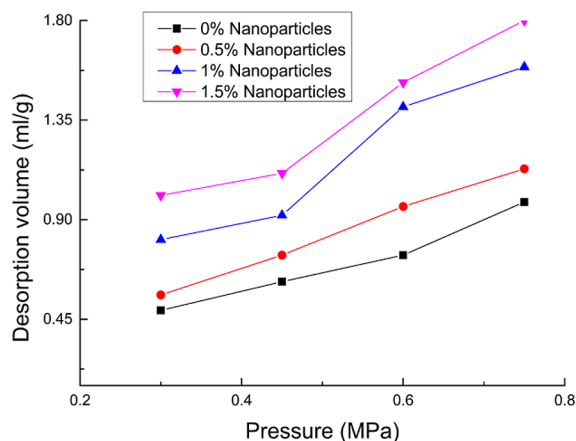
Figure 2. Methane adsorption capacity of different coal ranks.

Table 1. Methane Adsorption Capacity of Different Coal Rank Coals

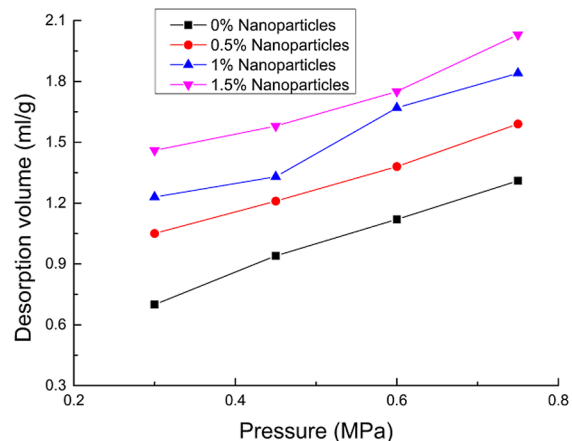
coal rank	mass fraction of nanoparticles (%)	adsorption volume at different equilibrium pressures (mL/g)			
		0.3 MPa	0.45 MPa	0.6 MPa	0.75 MPa
low-rank coal	0	1.18	1.51	1.71	2.03
	0.5	1.42	1.67	2.07	2.35
	1	1.61	1.84	2.25	2.60
	1.5	1.87	2.11	2.54	2.91
medium-rank coal	0	1.66	1.96	2.25	2.54
	0.5	1.81	2.13	2.37	2.67
	1	1.95	2.34	2.65	3.08
	1.5	2.09	2.58	2.91	2.65
high-rank coal	0	4.66	4.93	5.16	5.35
	0.5	5.25	5.62	6.12	6.61
	1	5.86	6.24	6.58	6.97
	1.5	6.29	6.62	6.81	7.24

desorption tube were measured and recorded, and a stopwatch was prepared. Then, the desorption valve of the coal sample was opened within a short time, and the free gas in the

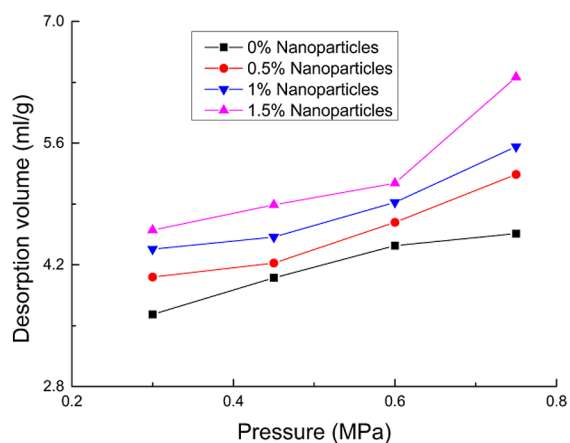
remaining space of the coal sample was released quickly. When the pointer of the pressure gauge of the coal sample dropped to zero, the three-way valve was quickly turned on the desorption



a. Desorption capacity of low-rank coal



b. Desorption capacity of medium-rank coal



c. Desorption capacity of high-rank coal

Figure 3. Methane desorption capacity of different coal rank coal.

Table 2. Methane Desorption From Different Coal Rank Coals

coal rank	mass fraction of nanoparticles (%)	adsorption volume at different equilibrium pressures (mL/g)			
		0.3 MPa	0.45 MPa	0.6 MPa	0.75 MPa
low-rank coal	0	0.49	0.62	0.74	0.98
	0.5	0.56	0.74	0.96	1.13
	1	0.81	0.92	1.41	1.59
	1.5	1.01	1.11	1.52	1.80
medium-rank coal	0	0.7	0.94	1.12	1.31
	0.5	1.05	1.21	1.38	1.59
	1	1.23	1.33	1.67	1.84
	1.5	1.46	1.58	1.75	2.03
high-rank coal	0	3.63	4.05	4.42	4.56
	0.5	4.06	4.22	4.69	5.24
	1	4.38	4.52	4.92	5.56
	1.5	4.6	4.89	5.14	6.36

instrument to connect the coal sample with the desorption glass tube, and the stopwatch was immediately pressed to start timing. The amount of methane desorption in the glass tube was accurately read and recorded at the corresponding moment within 120 min.

The methane desorption experiments were conducted on clean fracturing fluid- and nanofracturing fluid-treated coal samples at 30 °C. The methane desorption test results of different coal samples are shown in Figure 3.

From Figure 3 and Table 2, it can be seen that the methane desorption amounts of the three different coal rank coal

samples treated with normal clean fracturing fluid and nanofracturing fluid showed an increasing trend with pressure, the reason for the large variation of desorption at 0.4–0.6 MPa for four coals with different nanoparticle contents in the desorption diagram of low-rank coal is that there is a competitive adsorption relationship between nanoparticles and fracturing fluid, and breaking the critical value in this interval causes an increase in the rate of change of desorption. The results of methane isothermal desorption experiments show that the methane adsorption amounts of coal samples treated with different mass fraction nanofracturing fluids are higher than those treated with normal clean fracturing fluids. At an adsorption equilibrium pressure of 0.75 MPa, the nanoparticle mass fractions of 0.5, 1.0, and 1.5% compared to the methane adsorption of coal samples after treatment with normal clean fracturing fluid: the increase of gas adsorption of low-rank coal was 15.31, 62.24, and 83.67%; the increase of gas adsorption of middle-rank coal was 21.37, 40.46, and 54.96%; and the increase of gas adsorption of high-rank coal was 14.91, 21.93, and 32.23%.

3.2. Molecular Simulation Study of Coal Methane Adsorption Diffusion after Nano Fracturing Fluid Treatment.

3.2.1. Simulation Scheme. Materials Studio (MS) software was used for molecular simulations and molecular dynamics simulations. First, we construct a planar model of raw coal and perform geometry optimization and annealing simulation to find the lowest energy configuration of raw coal molecules. Then, density optimization is conducted to model the optimal spatial structure of coal molecules and to model the slit pores of coal with different pore sizes. Subsequently, clean fracturing fluid and nanofracturing fluid system-treated coal structure models with different pore sizes were established, and methane adsorption and diffusion molecular simulation studies were also conducted on them; additionally, methane adsorption and diffusion coefficients of coal structure models under both systems were calculated, and the effects of methane adsorption by coal molecules and diffusion ability of methane molecules in coal after nanofracturing fluid treatment were studied as microscopic pattern analysis of the previous adsorption; desorption experiments were used for in-depth explanations of the source of the enhanced gas adsorption and desorption ability caused by nanofracturing fluid.

3.2.2. Construction of the Coal Model. The construction of molecular structure models of coal is derived by extrapolation of various structural parameters of coal,¹⁸ which vary from one type of coal to another, making it difficult to unify the variety of molecular models of coal. Huang Qiming used ¹³C NMR experiments and combined them with ACD Labs software to optimize the construction of the molecular structure model of a coal sample from the Illinois Basin, USA. This coal sample belongs to the high-rank coal, and we compared the waveform diagram of the mapped coal sample with the waveform diagram obtained from the actual NMR experiments, both of which are in good agreement, and concluded that the mapped coal molecular structure is consistent with the structure of coal in the real coal seam.¹⁹ In this paper, the molecular structure of Illinois Basin coal constructed by Huang Qiming was used for molecular simulation studies. After determining the chemical formula of coal molecules, the Visualizer tools module in the Materials Studio software draws the chemical formula of coal molecules into the initial molecular structure model of coal samples and performs energy minimization on the initial coal

molecular structure model to meet the calculation requirements, including geometry optimization and anneal. The amorphous cell module in MS software is used to impose periodic boundary conditions to construct a single coal molecule spatial model, and the density value set by the amorphous cell module is continuously altered to calculate the system energy of the single molecule spatial structure at separate densities. The lowest energy obtained is the optimal density of coal molecules and the optimal spatial structure model, and the constructed model is shown in Figure 4.

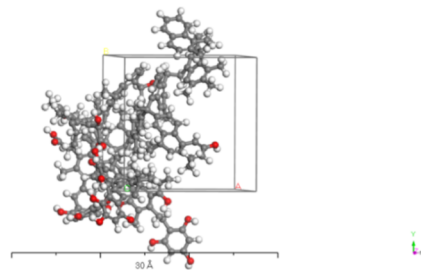


Figure 4. Spatial structure model of coal molecules under optimal density.

In the previous methane adsorption–desorption experiments, by fixing the mass fraction of clean fracturing fluid constant and changing the mass fraction of nano-silica, the changes in liquid nitrogen and methane adsorption capacity of coal samples after nano clean fracturing fluid treatment were investigated, and the change pattern and influencing factors of methane adsorption–desorption capacity of coal after nanofracturing fluid treatment were derived. In this section, molecular simulations are used to compare and analyze the results with those obtained in the previous paper. In the molecular simulation, hexadecyl trimethyl ammonium bromide (CATB) and CATB + SiO₂ were added to the coal pore structure in the form of adsorption using the Sorption module in MS to simulate the coal samples after clean fracturing fluid treatment and after nanofracturing fluid treatment, respectively. Methane adsorption and diffusion simulations were carried out on two separate systems of coal samples to study the effect of the nanofracturing fluid on the adsorption and diffusion capacity of methane in coal. The clean fracturing fluid- and nanofracturing fluid-treated coal samples are shown in Figures 5 and 6.

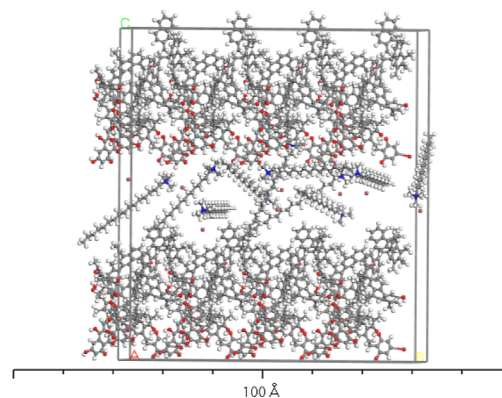


Figure 5. Molecular model of coal after clean fracturing fluid treatment.

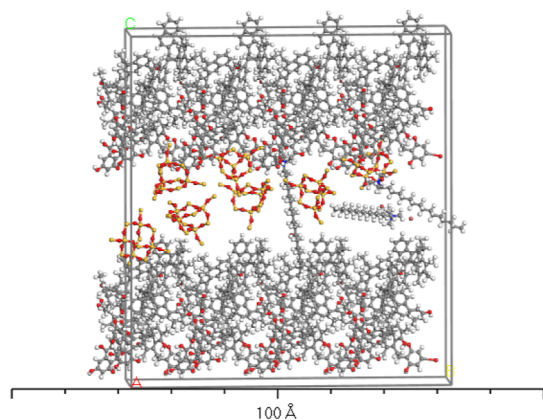


Figure 6. Molecular model of coal after nanofracturing fluid treatment.

3.2.3. Analysis of Isothermal Adsorption Results. The methane adsorption by coal molecules is simulated using the Sorption module in Materials Studio. Then, the compass force field is selected in the energy section of the software, the maximum equilibrium step is set to 10,000, the maximum loading step is set to 100,000, the simulation temperature is set to 303.15 K, the simulation accuracy is set to fine, Electrostatic Ewald is selected and atom based is selected for van der Waals. The simulated pressures were set to 0.3, 0.45, 0.6, 0.75, 1, 2, 4, 6, 8, and 10 MPa to study the change pattern of methane adsorption by coal after treatment of the two systems.

The expression for the potential energy function of the COMPASS force field is as follows

$$\begin{aligned}
 E_{\text{total}} = & \sum b[k_2(b - b_0)^2 + k_3(b - b_0)^4]^2 \\
 & + \sum i[k_2(i - i_0)^2 + k_3(i - i_0)^3 + k_4(i - i_0)^4]^2 \\
 & + \sum \phi[k_1(1 - \cos \phi) + k_2(1 - \cos 2\phi) \\
 & + k_3(1 - \cos 3\phi)] + \sum \chi k_2 \chi^2 \\
 & + \sum b, b' k(b - b_0)(b' - b'_0) \\
 & + \sum b, ik(b - b_0)(i - i_0) \\
 & + \sum b, \phi(i - i_0)[k_1 \cos \phi + k_2 \cos 2\phi \\
 & + k_3 \cos 3\phi] + \sum b, ik(i' - i'_0)(i - i_0) \\
 & + \sum i, j, \phi k(i' - i'_0)(i - i_0) \cos \phi + \sum i, j \frac{q_i q_{ij}}{r_{ij}} \\
 & + \sum i, j \epsilon_{ij} \left[2 \left(\frac{r_{ij}^0}{r_{ij}} \right)^9 - 3 \left(\frac{r_{ij}^0}{r_{ij}} \right)^6 \right] \quad (1)
 \end{aligned}$$

where k_2 , k_3 , and k_4 are the elastic constants of chemical bonds; b is the chemical bond length; b_0 is the equilibrium bond length; i is the bond angle; i_0 is the bond angle at equilibrium; ϕ is the two-sided angle; ϵ_{ij} is the effective permittivity; q_i , q_{ij} are the charges of atoms; and r_{ij} is the distance between two atoms.

As shown in eq 1 above, the first, second, and third terms in its expression are the bond angle stretching, bending, and twisting energies, respectively; the fourth term is the out-of-plane bending angle energy; from the fifth to the eleventh terms are the cross-coupling energies of the bonds,

respectively, the latter two terms are the nonbonding forces, the twelfth term is the Coulomb force and the thirteenth term is the van der Waals force. The COMPASS force field combines the hydrogen bonding forces with the other nonbonding forces together and therefore cannot be represented in isolation.

The equation for fugacity (ideal gas) is as follows

$$f = \varphi \times P \quad (2)$$

where f (MPa) is the fugacity, φ is the fugacity coefficient, and P (MPa) is the pressure.

At the end of the simulation, Materials Studio generates a file, which represents the absolute amount of methane molecules adsorbed by the coal molecules of the system, with the following equation.

$$N_{\text{abs}} = \frac{1000 \times N_{\text{am}}}{N_a \times M_s} \quad (3)$$

where N_{abs} (mmol/g) is the absolute adsorption amount; N_{am} (molecules/u.c) is the number of adsorbed molecules; N_a is the number of cells; and M_s (mol/g) is the molar mass of cells.

The absolute adsorption amount contains the gas molecules adsorbed on the pore wall of the porous material in the form of the adsorbed phase and the gas molecules present inside the pores of the porous material in the form of gas. In contrast, our actual analysis is performed with the excess adsorption amount for the analysis of the results, so a conversion is needed, and the conversion equation is shown below^{20,21}

$$N_{\text{exc}} = N_{\text{abs}} - V_p \times \rho \quad (4)$$

where N_{exc} is the excess adsorption volume, N_{abs} is the absolute adsorption volume, and V_p is the pore volume of the adsorbent, which can be approximated as the free volume of the adsorbent (since the free volume contains the volume of closed pores, closed pores are not considered in this paper), and ρ (kg/m³) is the density of methane gas at each pressure. The density of methane can be calculated from the Peng–Robinson equation of state, which is as follows

$$P = \frac{RT}{V_m} - \frac{a\alpha}{V_m^2 + 2bV_m + b^2} \quad (5)$$

$$\begin{aligned}
 \text{where } a &= \frac{0.45724R^2T_c^2}{P_c}, b = \quad, P_c \text{ is the} \\
 &= \frac{0.07780RT_c}{P_c}, \alpha \\
 &= [1 + \kappa(1 - T_c^{0.5})^2], \kappa \\
 &= 0.37464 + 1.54226\omega - 0.2699\omega^2, T_r \\
 &= \frac{T}{T_c}
 \end{aligned}$$

critical pressure, T_c is the critical temperature, T_r is the specific temperature, and ω is the acentric factor. The parameters of methane in the critical state are $T_c = 190.56$, $P_c = 4.5990$ MPa, and $\omega = 0.0115$.

The calculated results are shown in Table 3 for the molecular adsorption amounts for different pore-size coal structures in both systems.

As shown in Table 3, the total number of adsorbed molecules of the CATB + SiO₂ system (nanofracturing fluid) at 1, 2, 4, and 10 pore sizes is 8.552, 14.365, 27.061, and 58.887 mmol/g, respectively, which are near equal to the total number of adsorbed molecules of coal in the CATB system. In

Table 3. Molecular Adsorption Capacity of Two Systems by Coal Structures With Different Pore Sizes

pore size nm	adsorption capacity of different systems molecular/u.c		
	CATB	CATB + SiO ₂	
	CATB	CATB	SiO ₂
1	8.233	2.913	5.639
2	14.096	9.946	4.419
4	27.054	8.632	18.429
10	58.627	29.45	29.437

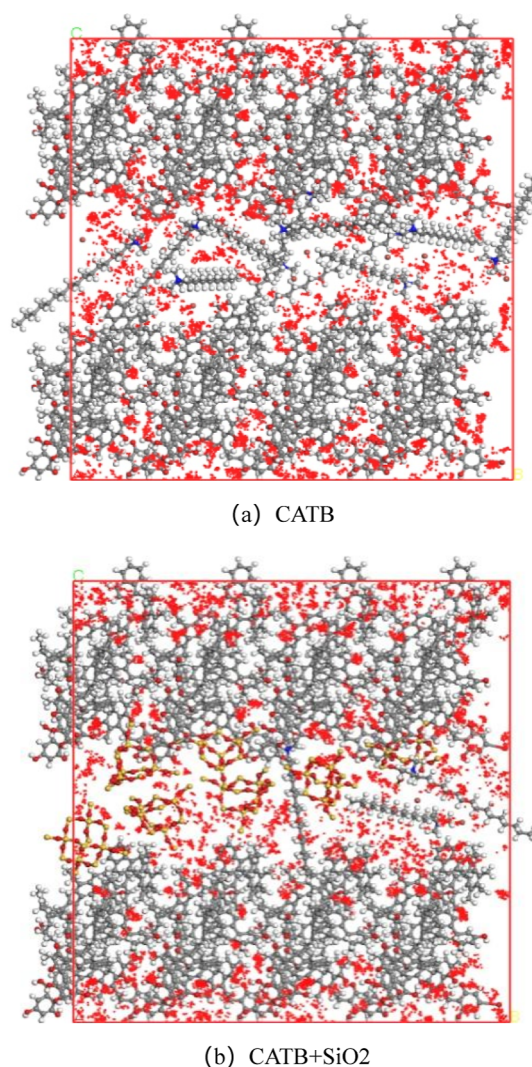
contrast, the adsorption of CATB molecules in the CATB + SiO₂ system by coal is significantly smaller than that in the CATB system, indicating that there is a competitive adsorption between SiO₂ in CATB + SiO₂ and CATB in the system, i.e., the nanoparticles in the nanofracturing fluid can hinder the adsorption of surfactant molecules in the clean fracturing fluid by coal. The decrease of CATB adsorption in the CATB + SiO₂ system at 4 nm pore size is due to the presence of competitive adsorption, which decreases the amount of CATB adsorption compared to the adjacent pore size when the amount of SiO₂ adsorption increases suddenly and substantially.

Figure 7a,b shows the 1 nm pore-size coal methane isothermal adsorption models after treatment with different systems.

The red dots in Figure 7 are the density distribution of methane; the denser the dots, the denser the color and higher the probability that methane is distributed at that location. It can be seen from the figure that methane molecules are not uniformly distributed in the coal molecular model but are mainly concentrated on the surface of coal molecules and pore wall surfaces and are also partly distributed in the pore space (free space). The same conclusion was obtained at 2, 4, and 10 nm pore sizes. The simulation results are shown in Figure 8, which plots the absolute and excess methane adsorption after treatment with different fracturing fluid treatments.

From Figure 8, it can be seen that the excess adsorption of the 1, 2, 4, and 10 nm coal slit pore models increased faster at 0–2 MPa, and the excess adsorption increased slower after 2 MPa. The growth curve of excess adsorption became flat and horizontal with the increase in pore size from 2 to 6 MPa. The excess adsorption reached the maximum value at 6 MPa, and the excess adsorption of the 1, 2, 4, and 10 nm coal slit pore models showed a decreasing trend when the pressure continued to increase in the pressure interval from 6 to 10 MPa. This is because the critical temperature of methane is 190.56 K, and the critical pressure is 4.599 MPa, while the temperature set in this simulation is 303.15 K. At this temperature, the methane molecules are supercritical and do not coalesce and liquefy, increasing with increasing pressure, and when the two densities are equal, the excess adsorption amount reaches the maximum, which explains why the excess adsorption of each section pore size coal slit pore model is maximum at 6 MPa, while the free phase gas density is greater than the adsorbed phase gas density with a further increase in pressure, which leads to a decrease in the excess adsorption of each section pore size coal slit pore model at 6 to 10 MPa.

The gel formation principle of the clean fracturing fluid is that the hydrophilic groups in surfactants interact with water to form different types of micelle structures, while nanoparticles are added to form a more stable micelle structure, and the fracturing fluid will block the pore structure of coal rock in the

**Figure 7.** Density distribution of 1 nm CH₄.

form of adsorption and retention. Some of the permeable pores open at both ends in the coal after nanofracturing fluid treatment become open at one end, and some of the permeable pores that were open at one end close. The reason for the enhanced methane adsorption capacity of coal samples may be related to the increase in specific surface area, which makes more methane adsorption sites on the coal surface and enhances the methane adsorption capacity of coal, explaining the reason for the enhanced gas adsorption and desorption capacity of nanofracturing fluid in the previous adsorption and desorption experiment.

3.2.4. Analysis of the Methane Isothermic Heat of Adsorption Results. The adsorbent and the adsorbent mass are attracted to each other by intermolecular forces (van der Waals forces), resulting in the phenomenon of adsorption. Intermolecular kinetic energy is reduced and intermolecular kinetic energy is released in the form of heat energy, so adsorption is an exothermic process, generating heat. To better describe the adsorption characteristics of different systems on coal molecules, the isothermic heat of adsorption is introduced for analysis. The isothermic heat of adsorption is calculated by treating the pressure, temperature, and specific surface area of the adsorbent as a constant that does not change and calculating the heat released when the adsorption of an

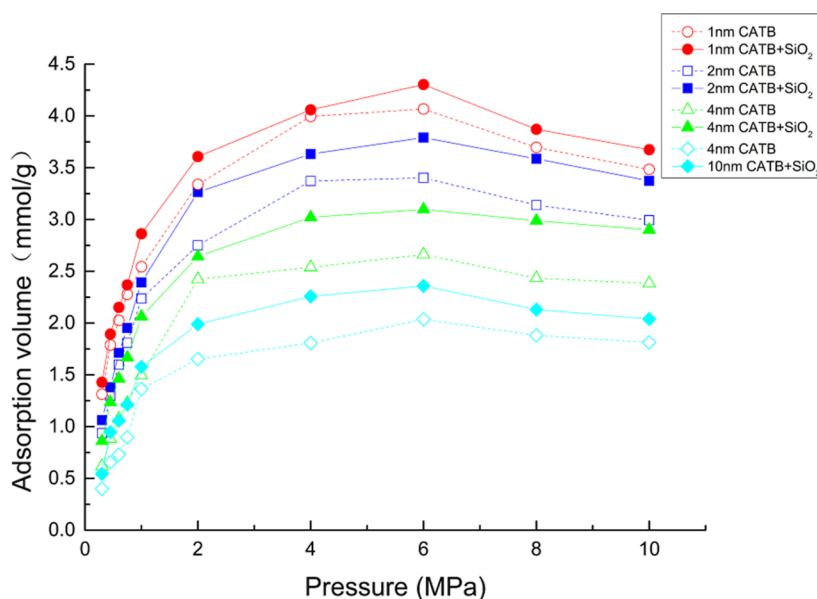


Figure 8. Methane adsorption capacity of coal after treatment with different systems.

Table 4. Isotheric Adsorption Heat of Methane Under Different Systems

CATB					CATB + SiO ₂				
pressure (MPa)	isotheric heat of adsorption (kJ/mol)				pressure (MPa)	isotheric heat of adsorption (kJ/mol)			
	1 nm	2 nm	4 nm	10 nm		1 nm	2 nm	4 nm	10 nm
0.3	16.986	16.568	15.333	13.922	0.3	16.693	16.426	15.128	14.421
0.45	17.007	16.463	14.961	13.680	0.45	17.024	16.199	14.944	13.893
0.6	16.761	16.158	14.927	13.575	0.6	16.643	15.944	14.839	13.022
0.75	16.464	16.909	14.822	13.190	0.75	16.731	15.806	14.676	13.554
1	16.916	16.363	14.517	13.069	1	16.426	16.300	14.383	12.897
2	16.392	15.58	14.322	12.818	2	16.526	15.689	14.291	12.458
4	16.727	15.656	14.278	12.951	4	16.526	15.409	14.274	12.638
6	16.325	15.898	14.191	12.964	6	16.564	15.526	14.542	12.684
8	16.585	15.844	14.542	12.914	8	16.685	15.990	14.551	12.918
10	16.731	15.66	14.425	13.073	10	16.618	15.689	14.638	13.094

infinitesimal adsorbate occurs on the surface of the adsorbent. The isotheric heat of adsorption is typically used to measure the strength of the force between the adsorbent and the adsorbate. Its equation is^{20,21}

$$q_{st} = T(v_g - v_a) \frac{dp}{dT} \quad (6)$$

where q_{st} (kJ/mol) is the isotheric heat of adsorption, v_g (m³/mol) is the molar volume of the bulk phase gas, and v_a (m³/mol) is the molar volume of the adsorbed phase gas.

The calculated results are shown in Table 4 for the isotheric heat of adsorption of 1 nm pore-size methane for different systems.

As seen from Table 4, the isotheric heat of adsorption of methane in both systems shows a decreasing trend with a gradual increase in pressure. This is because the magnitude of the isotheric heat of adsorption is related to the homogeneity of the distribution of the strong and weak adsorption sites on the solid surface and the intermolecular forces of the adsorbed gas. The isotheric heats of adsorption for both systems were less than 42 kJ/mol at each pressure, and it was inferred that the adsorption of methane molecules in both systems was physical. The isotheric heat of adsorption of methane in the CATB system with different pore sizes is greater than that in the

CATB + SiO₂ system, indicating that the force between methane and coal molecules in the CATB + SiO₂ system is smaller than that between methane and coal molecules in the CATB system, indicating that the adsorption of methane in the CATB + SiO₂ system is less stable than that in the CATB system, which makes methane desorption out more readily. We verified the previous phenomenon that the data of methane desorption experiments were elevated after treatment with nano clean fracturing fluid. We also found that the methane isotheric heat of adsorption gradually decreases as the pore size increases, indicating that methane does not easily form a stable adsorption structure with coal as the pore size increases, which can explain why large pores are an important site for methane desorption from coal.

3.2.5. Simulation Study of Methane Molecular Diffusion in Coal under the Action of Fracturing Fluid. Dynamics in the Forcite module of MS were used to simulate the molecular dynamics of the system. The NVT system was used for the simulation process, with the temperature set to 303.15 K and the step number to 100,000 to study the MSD curve of methane in 100 ps. The MSD curve of methane was obtained by analysis after the simulation was completed. The diffusion coefficients were calculated using the MSD curve and Einstein's method, where Einstein's algorithm equation is

$$D = \frac{1}{6N} \lim_{t \rightarrow \infty} \frac{d}{dt} \left\{ \sum_{i=1}^N [r_i(t) - r_i(0)]^2 \right\} \quad (7)$$

where D (m^2/s) is the diffusion coefficient, N is the number of molecules of the adsorbate, t (ps) is the simulation time, $r_i(0)$ is the vector position of the initial moment of the adsorbate, and $r_i(t)$ is the position vector of adsorbate i at moment t .

Figure 9 shows the mean square displacement of coal methane at different pore sizes after fracturing fluid treatment

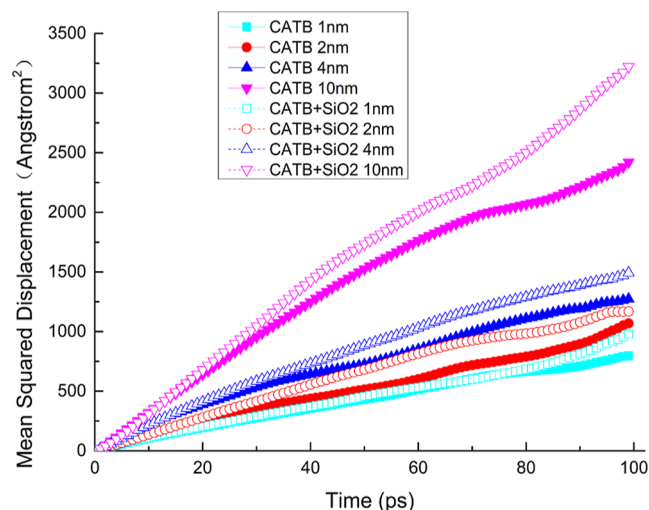


Figure 9. Mean square displacement of coal methane under different pore sizes after treatment with different systems.

for different systems, and Table 5 shows the diffusion coefficients of CH_4 at 1 MPa for different pore sizes.

Table 5. Diffusion Coefficient of CH_4 Under 1 MPa for Different Pore Sizes

System	diffusion coefficient of CH_4 at different pore sizes $D \times 10^{-8} \text{ m}^2/\text{s}$			
	1 nm	2 nm	4 nm	10 nm
CATB	1.30	1.61	2.05	4.03
CATB + SiO_2	1.46	1.99	2.47	5.26

From Figure 9, with the increase in pore size, the maximum mean square displacement of coal methane shows an increasing trend for both systems after treatment, which indicates that the increase in pore size is beneficial to the diffusion of methane molecules, which proves that the larger the pore size is, the easier methane desorption is combined with Table 5, it is found that the methane diffusion coefficient of the CATB + SiO_2 system increases 12.31, 23.62, 20.49 and 30.52% compared to the CATB system at 1, 2, 4 and 10 nm pore sizes, respectively, and methane is more easily desorbed from coal, the results corroborate with the previous Experimental Section in which the amount of desorption gradually increased after the addition of nano-illustrated nanoparticles to isothermal desorption, indicating that nano-particle-modified clean fracturing fluid can reduce the damage to methane desorption–diffusion in coal reservoirs.

4. CONCLUSIONS

- (1) The methane adsorption and desorption of coal samples treated with nano-fracturing fluid were greater than those treated with normal clean fracturing fluid, and the methane adsorption and desorption increased with increasing mass fraction of nanoparticles. As an example, when the adsorption capacity of coal was at 0.75 MPa, the nanoparticle mass fractions were 0.5, 1.0, and 1.5%, respectively, compared to the methane adsorption of coal samples after treatment with normal clean fracturing fluid; when the increase of gas adsorption for low-rank coal was 15.76, 10.63, and 11.92%, respectively, and the increase of gas adsorption for middle-rank coal was 5.12, 11.36, and 18.50%, respectively; the increase of gas adsorption for high-rank coal was 23.55, 5.45, and 3.87%, respectively.
- (2) Slit pore models of coal with different pore sizes were constructed after fracturing fluid treatment using MS software to carry out molecular simulations of methane adsorption and diffusion. The results showed that comparing the adsorption of surfactant in the fracturing fluid by the coal molecular model under two systems, it was found that the molecular number of surfactant adsorption in the CATB + SiO_2 system (nanofracturing fluid) under 1, 2, 4, and 10 nm pore sizes was 2.913, 9.946, 8.632, and 29.45 mmol/g, respectively; the total adsorption molecule numbers were 8.552, 14.365, 27.061, and 58.887 mmol/g, respectively; the adsorption molecule numbers of the CATB system (clean fracturing fluid) were 8.233, 14.096, 27.054, and 58.627 mmol/g. The adsorption of surfactant in the nanofracturing fluid was smaller than that of surfactant in clean fracturing fluid, while the overall adsorption did not change significantly; presumably, there was competitive adsorption between nanoparticles and surfactant.
- (3) The methane excess adsorption amount increased faster at 0–2 MPa, and the increase of excess adsorption amount slowed down with the increase of pore size at 2–6 MPa, with a horizontal-like trend, and the excess adsorption amount reached the maximum at 6 MPa; the excess adsorption amount gradually decreased with the increase of pressure at 6–10 MPa. The isothermal curve of gas adsorption derived by Materials Studio is basically consistent with the experimentally derived law and can be verified with each other.
- (4) The average isosteric heats of adsorption for the 1, 2, 4, and 10 nm coal slit pore models of the CATB system at 0.3–10 MPa were calculated to be 16.6894, 16.1099, 14.6318, and 13.2156 kJ/mol, respectively, while the average isosteric heats of adsorption for the CATB + SiO_2 system were 16.6436, 15.8978, 14.6266, and 13.1579 kJ/mol, respectively, the results show that the isosteric heat of adsorption of methane from coal with different pore sizes in the nanofracturing fluid system is smaller than that in the clean fracturing fluid system, indicating that the intermolecular force between coal and methane after the nanofracturing fluid treatment is smaller than that after the clean fracturing fluid treatment, making the methane easily desorbed.
- (5) Methane diffusion simulation using the molecular dynamics model for the coal molecular model after different fracturing fluid treatments show that the

methane diffusion coefficient tends to increase as the pore size increases, and the methane diffusion coefficient of the nano-fracturing fluid system increases by 12.31, 23.62, 20.49, and 30.52% compared to that of the clean fracturing fluid system under 1, 2, 4, and 10 nm pore sizes, respectively, which indicates that the methane diffusion ability of coal samples after nano-fracturing fluid treatment is stronger than that after clean fracturing fluid treatment, and comprehensively, nano-fracturing fluid is less harmful to the coalbed methane reservoir.

5. DISCUSSION

In the process of fracturing fluid acting on coal seams, the nano-fracturing fluid has the greatest effect on the adsorption and desorption of gas from coal seams. This paper provides a modified fracturing fluid formulation of 0.8% CATB + 0.2% NaSal + 1% KCl + SiO₂ (0.5, 1, 1.5%) and compares 6 MPa as the most suitable pressure for the nano-fracturing fluid to function. Future research could vary the type and particle size of SiO₂ nano added to clean fracturing fluids, analyzing the composition and specific chemical structure of different coal rank coals, and then optimizing them by using molecular simulation software and conducting gas adsorption and diffusion characteristics research.

AUTHOR INFORMATION

Corresponding Author

Huaizhen Li – School of Energy Science and Engineering, Henan Polytechnic University, Jiaozuo, Henan 454003, China; orcid.org/0009-0009-3585-013X; Email: 734556140@qq.com

Authors

Wei Qin Zuo – School of Safety Science and Engineering, Henan Polytechnic University, Jiaozuo, Henan 454003, China

Mingrui Qi – School of Safety Science and Engineering, Henan Polytechnic University, Jiaozuo, Henan 454003, China

Yanwei Liu – School of Safety Science and Engineering, Henan Polytechnic University, Jiaozuo, Henan 454003, China

Hongkai Han – School of Safety Science and Engineering, Henan Polytechnic University, Jiaozuo, Henan 454003, China; orcid.org/0000-0003-0042-6223

Yang Wang – School of Safety Science and Engineering, Henan Polytechnic University, Jiaozuo, Henan 454003, China

Liqun Long – School of Safety Science and Engineering, Henan Polytechnic University, Jiaozuo, Henan 454003, China

Shengjie Wu – School of Safety Science and Engineering, Henan Polytechnic University, Jiaozuo, Henan 454003, China

Complete contact information is available at:

<https://pubs.acs.org/10.1021/acsomega.3c02227>

Notes

The authors declare no competing financial interest.

ACKNOWLEDGMENTS

This project was supported by the National Natural Science Foundation of China (52274188, 52174173 and 52104190), the Universities of Henan Province (NSFRF210307), China Postdoctoral Science Foundation (2020M682291 and

2022T150194), “the Fundamental Research Funds for the Universities of Henan Province” (NSFRF210306), the Outstanding Youth Fund of Henan Polytechnic University of Technology (T2021-5 and J2021-5), the Focus R&D and Promotion for Scientific and Technological Project of Henan Province (222102320012), and the Strategic Research and Consulting Project of the Chinese Academy of Sciences (2023HENZDB05). The authors are grateful for their support.

REFERENCES

- (1) Luo, S. G.; Song, P. X.; Feng, D. W. Analysis on the status quo and comprehensive utilization of coalbed methane development and utilization in my country. *Int. J. Coal Prep. Util.* **2020**, *7*, 83–87.
- (2) Su, X. B.; Liu, B. M. The occurrence state of coalbed methane and its influencing factors. *Journal of Jiaozuo Institute of Technology* **1999**, *3*, 4–7.
- (3) Zhang, P. Research on fracturing fluid flow and proppant distribution in coalbed methane wells. Master's Thesis, China University of Petroleum: Beijing, 2011.
- (4) Zhao, H. Effect of Clean Fracturing Fluids on the Adsorption and Desorption Characteristics of Medium and High-Grade Coal. Master's Thesis; China University of Petroleum: Beijing, 2021.
- (5) Gu, J. Application of Clean Fracturing Fluids in Coalbed Methane Well Fracturing. *Chemical Engineering & Equipment* **2020**, *5*, 198–199.
- (6) Yang, M.; Ma, S. S.; Guan, C. Construction and performance evaluation of alcohol-based fracturing fluid systems. *Chin. J. Colloid Polym.* **2022**, *40*, 26–28.
- (7) Xiong, L. J.; Wang, L.; Wu, Y.; et al. Preparation and performance evaluation of high temperature resistant clean fracturing fluid. *Fine Chem.* **2022**, *39*, 204–211.
- (8) Wu, Y. Q. Rheological characterization of nanoparticle modified viscoelastic clean fracturing fluid. Master's Thesis, Zhejiang University: Hangzhou (Zhejiang), 2015.
- (9) Crawford, R. J.; Mainwaring, D. E. The influence of surfactant adsorption on the surface characterisation of Australian coals. *Fuel* **2001**, *80*, 313–320.
- (10) Nettesheim, F.; Liberatore, M. W.; Hodgdon, T. K.; Wagner, N. J.; Kaler, E. W.; Vethamuthu, M. Influence of nanoparticle addition on the properties of wormlike micellar solutions. *Langmuir* **2008**, *24*, 7718–7726.
- (11) Narkiewicz, M. R.; Mathews, J. P. Visual Representation of Carbon Dioxide Adsorption in a Low-Volatile Bituminous Coal Molecular Model. *Energy Fuels* **2009**, *23*, 5236–5246.
- (12) Qin, H. L. Study on the macromolecular structure of micro fractions of coal rocks in Hancheng mining area. Master's Thesis, Taiyuan University of Technology: Taiyuan (Shanxi), 2019.
- (13) Wang, L.; Li, Z.; Mao, G.; Zhang, Y.; Lai, F. P. Effect of Nanoparticle Adsorption on the Pore Structure of a Coalbed Methane Reservoir: A Laboratory Experimental Study. *ACS Omega* **2022**, *7*, 6261–6270.
- (14) Li, Y. Z.; DiCarlo, D.; Li, X.; Zang, J.; Li, Z. An experimental study on application of nanoparticles in unconventional gas reservoir CO₂ fracturing. *J. Petrol. Sci. Eng.* **2015**, *133*, 238–244.
- (15) Yang, J. C.; Li, F. C.; Zhou, W. W.; He, Y. R.; Jiang, B. C. Experimental investigation on the thermal conductivity and shear viscosity of viscoelastic-fluid-based nanofluids. *Int. J. Heat Mass Tran.* **2012**, *55*, 3160–3166.
- (16) Li, F. C.; Yang, J. C.; Zhou, W. W.; He, Y. R.; Huang, Y. M.; Jiang, B. C. Experimental study on the characteristics of thermal conductivity and shear viscosity of viscoelastic-fluid-based nanofluids containing multiwalled carbon nanotubes. *Thermochim. Acta* **2013**, *556*, 47–53.
- (17) Yao, Z.; Li, H. B.; Li, N. Study on the characteristics of coal-bed methane reservoirs in the Shanxi Group of the Hancheng Mining District. *Coal Technol.* **2021**, *40*, 96–99.
- (18) Lu, W. Y.; Huang, B. X.; Zhao, X. L. A review of recent research and development of the effect of hydraulic fracturing on gas

adsorption and desorption in coal seams. *Adsorpt. Sci. Technol.* **2019**, *37*, 509–529.

(19) Huang, Q. M. Study on the mechanism of the effect of water-based fracturing fluid on the flow of coal seam gas; Ph.D. Dissertation, China University of Mining and Technology: Beijing, 2020.

(20) Jhon, Y. H.; Cho, M.; Jeon, H. R.; Park, I.; Chang, R.; Rowsell, J. L. C.; Kim, J. Simulations of Methane Adsorption and Diffusion within Alkoxy-Functionalized IRMOFs Exhibiting Severely Disordered Crystal Structures. *J. Phys. Chem. C* **2007**, *111*, 16618–16625.

(21) Wang, B.; Zhang, L.; Zhang, R. Effects of coal molecular structure on the adsorption and diffusion behavior of coalbed methane. *CIESC J.* **2016**, *67*, 2548–2557.